

Journal of Nuclear Science and Technology

ISSN: 0022-3131 (Print) 1881-1248 (Online) Journal homepage: www.tandfonline.com/journals/tnst20

Beta-ray irradiation effect on optical and dielectric properties of InSe film

Cansu Emir , Sema Bilge Ocak , Adem Tataroğlu & Uğur Gökmen

To cite this article: Cansu Emir , Sema Bilge Ocak , Adem Tataroğlu & Uğur Gökmen (2026) Beta-ray irradiation effect on optical and dielectric properties of InSe film, Journal of Nuclear Science and Technology, 63:10, 1228-1236, DOI: 10.1080/00223131.2026.2691264

To link to this article: https://doi.org/10.1080/00223131.2026.2691264

Published online: 23 Jun 2026.

Submit your article to this journal

Article views: 64

View related articles

View Crossmark data

Full Terms & Conditions of access and use can be found at
https://www.tandfonline.com/action/journalInformation?journalCode=tnst20

JOURNAL OF NUCLEAR SCIENCE AND TECHNOLOGY
2026, VOL. 63, NO. 10, 1228–1236
https://doi.org/10.1080/00223131.2026.2691264

RESEARCH ARTICLE

Beta-ray irradiation effect on optical and dielectric properties of InSe film

Cansu Emir[a,b], Sema Bilge Ocak[a,c], Adem Tataroğlu[d] and Uğur Gökmen[e]

[a]Graduate School of Natural and Applied Sciences, Advanced Technologies, Gazi University, Ankara, Türkiye; [b]Physics Group, Atilim University, Ankara, Türkiye; [c]Basic and Engineering Sciences Central Laboratory Application and Research Center (GUTMAM), Gazi University, Ankara, Turkiye; [d]Department of Physics, Faculty of Science, Gazi University, Ankara, Türkiye; [e]Faculty of Technology, Department of Metallurgical and Materials Engineering, Gazi University, Ankara, Türkiye

ABSTRACT

In this study, the effects of β-ray radiation on the optical and dielectric properties of InSe thin film were investigated using a Sr-90 β-source at doses of 0, 5, 10, and 20 kGy. To analyze the optical properties of the film, the transmittance (T) and absorbance (A) measurements were performed using a UV–Vis spectrophotometer in the 500–1000 nm spectral range. Optical and dielectric parameters including absorption coefficient, extinction coefficient, optical band-gap, refractive index, dielectric constant and optical conductivity were obtained from T and A data. As the radiation dose increased, transmittance increased while absorbance decreased. Under β-irradiation, these dose-dependent changes confirm the occurrence of defect formation, band rupture, and local atomic rearrangements. The band-gap energy (E_g) InSe film, which has the direct optical transition, was determined from Tauc plot. The E_g values were found in the range of 1.67 eV (0 kGy) to 1.59 eV (20 kGy), that is, they were decreased with increasing radiation dose. These results demonstrate that the optical response of the InSe film is strongly dependent on both wavelength and irradiation dose.

ARTICLE HISTORY
Received 17 March 2026
Accepted 12 June 2026

KEYWORDS
Indium selenide (InSe); UV-Vis spectroscopy; beta radiation effect; optical constant; dielectric parameters

1. Introduction

In recent years, research into advanced semiconductor materials with superior optical and electronic properties has progressed rapidly. II-III – VI compounds (II = Zn, Cd, Hg; III = B, Al, Ga, In, Ti; VI = O, S, Se, Te, Po) are both the layered semiconductors and two-dimensional (2D) layered materials [1–3]. In addition, transition metal oxides (TMOs) such as NbO_2, MnO_2, TiO, NiO, MoO_3,WO_3, V_2O_5, Fe_3O_4 and Cr_2O_3 are used as layered, 2D, and thin-film semiconductors [4,5]. Among the layered III – VI semiconductors, indium selenide (InSe) has attracted particular attention due to its high carrier mobility, direct-to-indirect optical transitions, and band gap tunability ranging from 1.25 eV in bulk to 2.8 eV in the monolayer [6,7]. The layered structure of InSe, consisting of covalently bonded Se–In–In–Se sublayers held together by van der Waals interactions, eliminates surface dangling bonds and facilitates the fabrication of high-quality heterojunctions [8,9]. These features make InSe thin films promising for optoelectronic applications such as photodetectors, solar cells, and nanoscale transistors [10–12]. In recent years, thin-film InSe produced by deposition techniques such as molecular beam epitaxy, pulsed laser deposition, RF sputtering, and thermal evaporation has been extensively studied [13–15]. These films demonstrate high optical transparency in the visible region and direct allowed transitions, both of which are highly desirable for efficient energy conversion and optoelectronic device integration.

Radiation causes significant structural defects in semiconducting and metal-oxide thin films, particularly vacancy defects and oxygen vacancies, and this alters the optical and electrical properties of the film [16–20]. These radiation-induced defects typically act as trapping centers, modify the density of states within the band gap, and lead to a reduction in the optical band gap [21,22]. For instance, β-ray irradiation has been shown to decrease the absorption coefficient and shift the band edge in PbO thin films [21], while γ-irradiation has significantly affected the optical constants and dielectric behavior of In_2O_3 and phthalocyanine thin films [22,23]. In addition, the changes caused by radiation are primarily ionization damage (electron/hole generation) and displacement damage. Also, the radiation response of semiconducting thin films is crucial for the development, reliability and performance of devices operating under ionizing radiation. Especially, radiation effects play a crucial role in various applications such as space technology, nuclear medicine, and dosimetry.

The optical properties of materials describe how material interacts with electromagnetic radiation. This interaction includes transmission, transmittance, absorption, reflection, emission and scattering. The optical parameters also involve the absorption coefficient (α), refractive index (n), extinction coefficient

CONTACT Sema Bilge Ocak sbocak@gazi.edu.tr Graduate School of Natural and Applied Sciences, Gazi University, Ankara 06560, Türkiye
© 2026 Atomic Energy Society of Japan. All rights reserved.

(k), optical dielectric constant (ε) and optical conductivity (σ) [24–26]. These parameters are of fundamental importance for optical imaging and sensing devices, optical fibers, and sensor technologies. Radiation often causes changes in the optical and dielectric parameters of the material. Radiation, especially since it causes structural changes, can lead to a decrease in the absorbance and the absorption coefficient of materials. This decrease corresponds with an increase in the transmittance of material. The optical dielectric constant represents the electrical response of a material to ionizing and non-ionizing electromagnetic fields. The dielectric constant is complex and depends on the field frequency. The real part (ε_r) of the dielectric constant reflects the material's polarization under an external field, whereas the imaginary part (ε_i) of the dielectric constant is associated with optical losses [27]. Since dielectric parameters are directly related to the refractive index and extinction coefficient, changes in radiation-induced optical constants will consequently lead to changes in dielectric behavior. As irradiation dose increases, both ε_r and ε_i often decrease due to the suppression of long-range polarization and enhanced defect-mediated scattering [28,29].

In our previous study, we investigated the structural and optical properties of interfacial InSe thin films deposited by thermal evaporation [30]. The results obtained have confirmed that InSe film has the potential to be used in various optoelectronic and photovoltaic applications. This study focuses on investigating the radiation response and radiation dosimetry potential of InSe thin films. In this context, the InSe thin film was subjected to beta irradiation in the dose range of 0–20 kGy, and the radiation effects on the optical and dielectric properties of the film were investigated.

2. Experimental details

InSe thin film was deposited onto optically transparent glass substrates using the thermal evaporation technique under a vacuum pressure of 1×10^{-6} mbar, as reported in our earlier work [30]. Commercial optically transparent soda – lime glass substrates were used as the deposition substrates. The substrates were selected because of their high transparency in the investigated UV – Vis – NIR spectral range and their suitability for optical transmission measurements. Prior to deposition, the substrates were cleaned sequentially with acetone, ethanol, and deionized water in an ultrasonic bath for 15 min each, followed by drying in nitrogen flow to remove any surface contamination. High-purity (99.999%) indium and selenium powders were placed in an alumina-coated tungsten boat. During deposition, the substrates were rotated at a constant rate to ensure film homogeneity, and the evaporation rate was maintained at 2–3 Å/s as monitored by a quartz crystal thickness monitor. After deposition, the film was annealed at 250°C for 45 min in a nitrogen atmosphere to enhance crystallinity. The pristine InSe thin film used in this study was fabricated using the same thermal evaporation and annealing parameters reported in our previous study [30], where the crystal structure, morphology, elemental composition, and film thickness were confirmed by XRD, SEM, EDX, and profilometer measurements.

To examine the effects of radiation on the InSe film, it was exposed to β-irradiation using an Sr-90 source with an average energy of 0.546 MeV. The irradiation was conducted in air at room temperature, with total doses adjusted to 5, 10, and 20 kGy by varying the exposure time. The dose rate was calibrated using a standard ionization chamber, ensuring uniform exposure across the film surface. To avoid thermal effects, the film was mounted on aluminum sample holders with controlled spacing. The optical characterization of pristine and irradiated film was carried out using a HITACHI UV-2600 UV – Vis spectrophotometer in the spectral range of 500–1000 nm, with a step resolution of 1 nm. The irradiation level in the present study was characterized in terms of absorbed dose (kGy), which was determined using a calibrated ionization chamber. Although absorbed dose provides a direct measure of the energy deposited in the material, the electron fluence (electrons cm^{-2}) was not directly monitored during the irradiation process. Therefore, the irradiation effects discussed in this work are presented as a function of absorbed dose rather than particle fluence.

3. Research results and discussion

The UV-Visible (UV-Vis) spectroscopy is used to measure optical transmittance, absorbance and reflectance of a thin film as a function of wavelength. From transmittance (T) and absorbance (A) spectra, the absorption coefficient (α) was determined using Beer – Lambert's law, while the optical band gap (E_g) was obtained via Tauc plots. The extinction coefficient (k) and refractive index (n) were calculated from the measured optical spectra, and their dose-dependent variations were analyzed. Moreover, the UV-Vis spectra give important information about the complex optical dielectric constant (ε*) and optical conductivity (σ_{opt}) of a thin film.

There is an inverse logarithmic relationship between light absorption (absorbance) and light transmittance, which forms the basis of the fundamental principle of optics, the Beer-Lambert Law. This relationship is defined as $A = \log(1/T)$.

The optical transmittance (T) and absorbance (A) spectra as a function of wavelength (λ) of the InSe film in the 500–1000 nm range before and after beta-ray

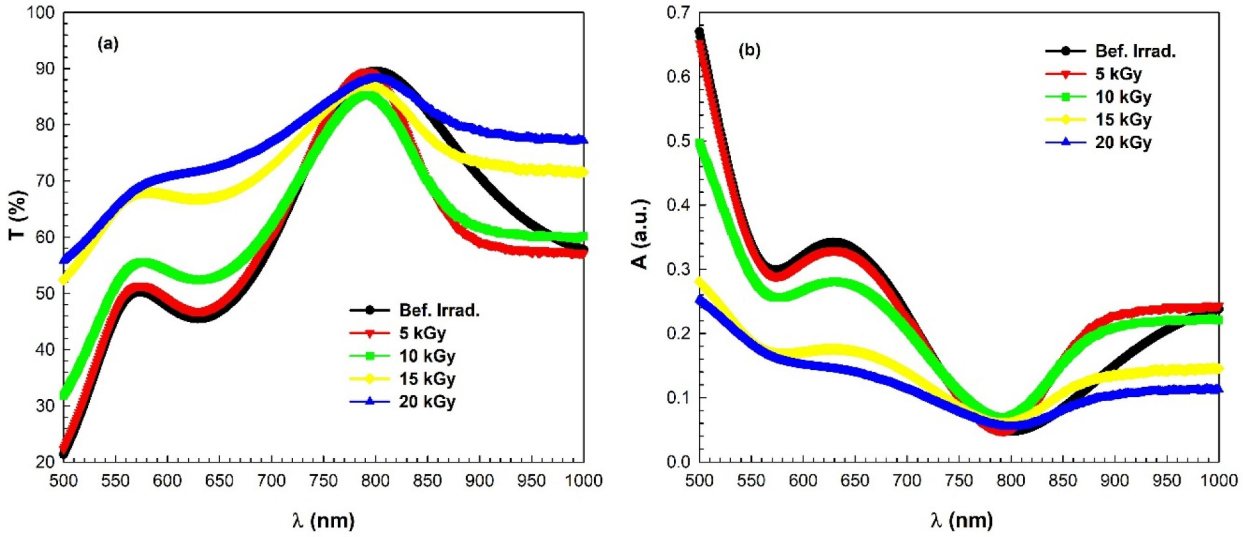

Figure 1. (a) Transmittance (T) (b) Absorbance (A) spectra of InSe film before and after beta-irradiation.

irradiation are illustrated in Figure 1(a,b), respectively. As seen in Figure 1(a), the transmittance spectrum indicates two peaks. The transmittance tends to increase in the range of 500 nm-575 nm and 625 nm-800 nm with wavelength. This may be due to the high absorption of photons by the film [31–34]. In addition, this film exhibits high transmittance in the near-infrared (NIR) region. Also, it is seen that radiation affects the transmittance and absorbance behavior at all spectra. In the wavelength range of 500 nm-750 nm, the transmittance changes significantly with radiation doses and increases with the increasing dose [35–38]. Additionally, as the irradiation dose increases, the transmittance peak becomes lower and its intensity decreases. Compared to the pre-radiation level in the range 750 nm-850 nm, transmittance decreases with radiation up to 10 kGy and then increases. After from 850 nm, transmittance decreases with radiation up to 5 kGy and then increases. Radiation energy can cause localized heating in the material, the release of trapped electrons, and the recombination of defects, thus increasing light transmittance. The decrease in transmittance can be attributed to defects caused by radiation. At the same time, bond breaks and bond rearrangements occur in the structure of thin films as a result of irradiation. As seen in Figure 1(b), in the range of 500–750 nm, the optical absorbance decreases as the radiation dose increases up to 20 kGy. Radiation can cause changes in the crystal structure of materials by displacing atoms and creating point defects and line defects. This can reduce absorption by eliminating light-absorbing centers. At the same time, bond breaks and bond rearrangements occur in the structure of thin films as a result of irradiation. Besides, from Figure 1(b), it is seen that the absorption peak is in the range of 600–700 nm. Also, a maximum absorption band was observed at about 625 nm. As a result, the behavior of transmittance and absorbance depending on the irradiation dose is consistent with the results in the literature [19–23,27–29,35–37].

Determining the absorption coefficient (α) provides a means to calculate the band gap of a material. The absorption coefficient was extracted from the following equations, respectively [35–39]

$$\alpha = \frac{1}{d}\ln\left(\frac{1}{T}\right) \text{ or } \alpha = \frac{2.303*A}{d} \quad (1)$$

Here, there is a relationship between absorbance and transmittance: A = log (1/T). That is, the absorbance value is inversely proportional to the transmittance value. Besides, d is the thickness of the InSe film (about 637 nm). The change of the absorption coefficient with respect to wavelength before and after irradiation is given in Figure 2(a). It was found that the α value decreased as irradiation dose increased.

Optical absorption is one of the most common methods used to determine the optical constants and band gap of thin films. The optical energy band gap (E_g) of the irradiated InSe film can be determined by the Tauc approximation given below [40],

$$(\alpha\ h\nu) = A\left(h\nu - E_g\right)^n \quad (2)$$

Here, E = hν is the energy of the incident photons, A is a constant, and the exponent n characterizes the electronic transition and takes the values 1/2 and 2 for direct and indirect allowed transitions, respectively [41–44]. Because InSe has direct allowed energy gap, the *n* value is taken as 1/2 [30,44,45]. Thus, the band gap is obtained from the plot $(\alpha h\nu)^2$ against by extrapolating the curves to hν axis at $(\alpha h\nu)^2 = 0$. Figure 2(b) demonstrates the plot of $(\alpha h\nu)^2$ versus hν for the InSe film before and after radiation. In the dose range of 0–20 kGy, the values of the direct band gap are found to be 1.67 ± 0.01, 1.66 ± 0.01, 1.64 ± 0.02, 1.61 ± 0.01 and 1.59 eV±0.02, respectively. The reduction of the

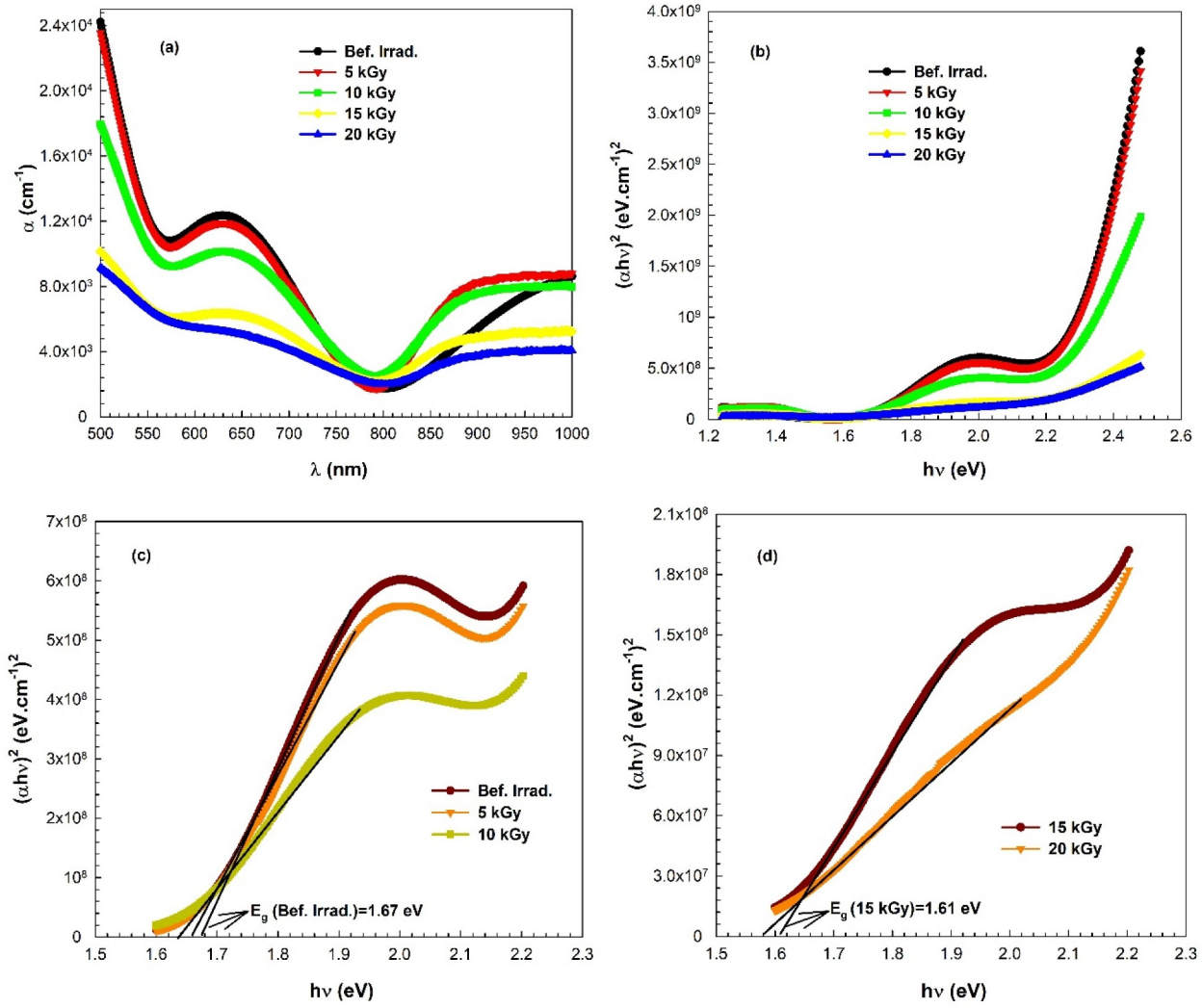

Figure 2. Variation of (a) the absorption coefficient (α) with the wavelength (λ) and (b) $(\alpha h\nu)^2$ with photon energy (hν) before and after radiation (c) $(\alpha h\nu)^2$vs hν plots for 0–5-10 kGy (d) $(\alpha h\nu)^2$vs hν plots for 15–20 kGy.

optical band gap with increasing irradiation dose is commonly observed in various materials, particularly polymers, thin films, and glasses exposed to ionizing radiation. This is caused by radiation-induced structural defects and localized states.

In other words, defects cause a reduction in the optical energy band gap by creating localized conditions in the film band structure [20,33,37,38].

The following equations are used to calculate the optical constants such as extinction coefficient (k) and refractive index (n), respectively [28,29,37,39].

$$k = \frac{\alpha\lambda}{4\pi} \tag{3}$$

and

$$n = \left(\frac{1+R}{1-R}\right) + \sqrt{\frac{4R}{(1-R)^2} - k^2} \tag{4}$$

where R is the reflectance. The *R* value can be obtained from the transmittance and the absorbance data by using the equation, A+R+T = 1 [32–34]. Figure 3(a,b) shows the variation of the extinction coefficient and refractive index with wavelength before and after radiation. As clearly seen in these figures, the *n* value is greater than the k value. Additionally, from these figures, as the radiation dose increases, there is a decrease in the extinction coefficient and refractive index values in the range 500–750 nm [22,23,35]. The decrease in k and *n* values can be ascribed to the decrease in localized states. Besides, the extinction coefficient exhibits the same behavior with the absorption coefficient.

Furthermore, optical electronegativity (η_{opt}) is used to evaluate differences in the physicochemical parameters of semiconductor materials. The η_{opt} of InSe films was calculated using the following formula [46,47]:

$$\eta_{opt} = \left[\frac{A}{n}\right]^{1/4} \tag{5}$$

Here, A is a dimensionless constant, taken as 25.54 for all materials. Figure 3(c) shows the variation of optical electronegativity (η_{opt}) with the wavelength. As seen in this figure, η_{opt} curves exhibit behavior

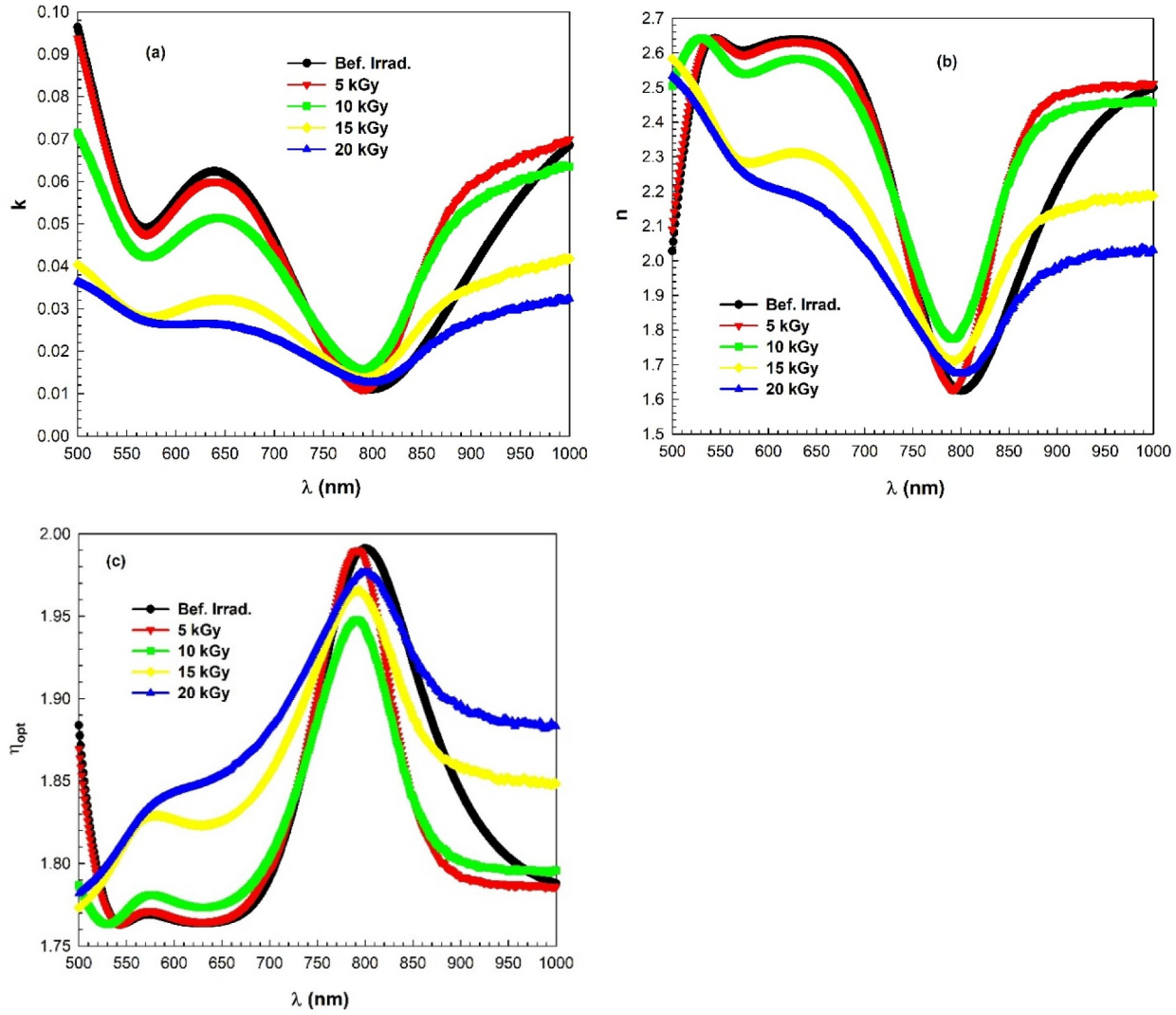

Figure 3. Variation of (a) the extinction coefficient (k) and (b) refractive index (n) (c) optical electronegativity (η_{opt}) with the wavelength before and after radiation.

inversely to refractive index curves. Optical electronegativity increases with increasing radiation.

Other optical constants like optical dielectric constant and optical conductivity of the materials used in photovoltaic devices must also be taken into account. The optical dielectric constant provides a comprehensive description of light transmission, reflection, and absorption (loss). The optical dielectric constant determines the refractive index of a material. Both the refractive index and the dielectric constant are complex functions consisting of real and imaginary parts. The relationship between the complex refractive index (n*) and the complex optical dielectric constant (ε*) is defined by the equation given below.

$$n^* = n + ik = \sqrt{\varepsilon^*} = \sqrt{\varepsilon_r + i\varepsilon_i} \quad (6)$$

where n and k, ε_r and ε_i are the real and imaginary components of n* and ε*, respectively. The ε_r represents the polarization of the material under the electromagnetic field whereas the ε_i describes the optical loss. The ε_r and ε_i are determined using the following relations [45,48–51].

$$\varepsilon_r = n^2 - k^2 \text{and } \varepsilon_i = 2nk \quad (7)$$

Figure 4(a,b) display the variation both ε_r and ε_i with wavelength before and after beta radiation. It is seen from the graphs that their values after irradiation were decreased in the range 500–750 nm. Additionally, the ε_r values are higher than the ε_i values.

Optical conductivity is a measure of the movement of charge carriers under the influence of incident electromagnetic radiation. The optical conductivity (σ_{opt}) was determined by the following equation [52–57]:

$$\sigma_{opt} = \frac{\alpha nc}{4\pi} \quad (8)$$

where c is the velocity of light in vacuum. Figure 5 indicates the variation of optical conductivity (σ_{opt}) with photon energy (hυ). In the range of 500 nm-575 nm and 625 nm-800 nm with wavelength, it is observed that optical conductivity increases as photon energy rises. This increase is due to the electrons being excited by the incoming photon energy [58]. Moreover, as the radiation dose increases, the σ_{opt}

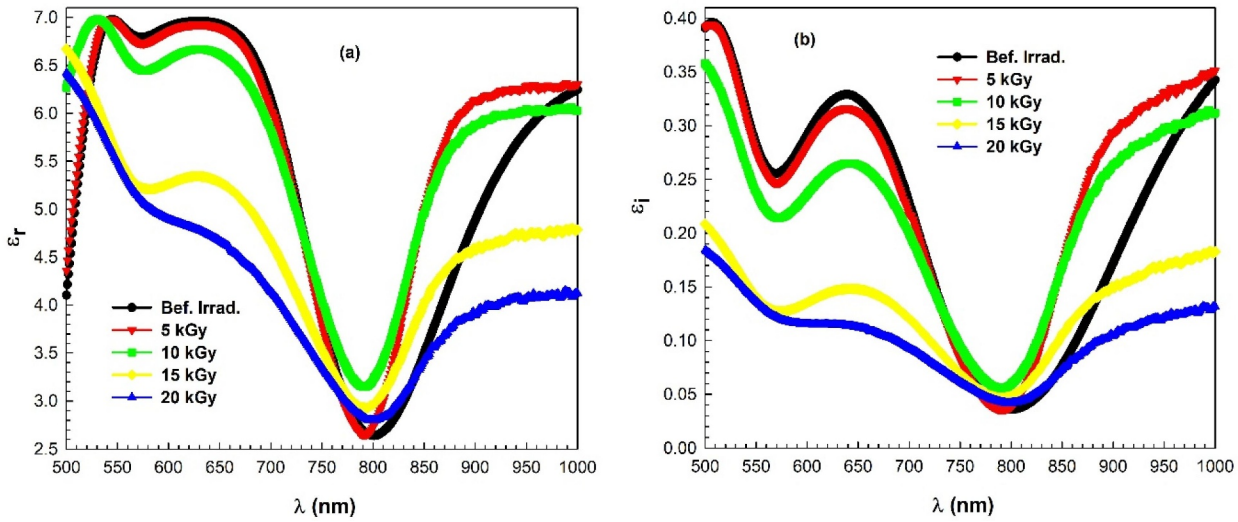

Figure 4. Variation of (a) real (ε_r) and (b) imaginary (ε_i) parts of the complex dielectric constant with wavelength before and after radiation.

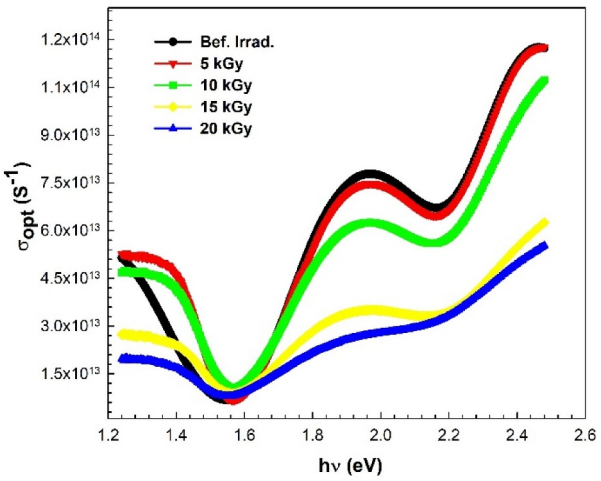

Figure 5. σ_{opt}-hν plot.

value decreases. Radiation-induced damage often results in defects and charge carrier trapping in materials. As radiation exposure increases, this leads to a decrease in optical conductivity. In addition, these plots exhibit an indication of a peak in the visible region. The peak is directly related to the electronic transitions between the bands.

The structural and morphological properties of thermally evaporated InSe thin films prepared under identical deposition and annealing conditions were comprehensively investigated in our previous study using XRD, SEM, and EDX analyses [Ref. 30]. In the present work, the same fabrication procedure was employed, while the main focus was the investigation of β-irradiation-induced changes in optical and dielectric parameters.

4. Conclusion

In this study, the influence of β-ray irradiation on the optical and dielectric properties of InSe thin film was comprehensively investigated in the 0–20 kGy dose range. The InSe film was subjected to controlled irradiation using a Sr-90 β-source. The analysis of transmittance and absorbance spectra revealed that the optical response of InSe film is highly sensitive to both the irradiation dose and the spectral region. The extinction coefficient (k) and refractive index (n) decrease with increasing radiation dose in the wavelength range of 500 nm-750 nm. The optical band gap (E_g) was determined using the commonly used Tauc graph. It was found that the obtained E_g value decreased as the irradiation dose increased. In addition, dielectric analysis revealed that both the real (ε_r) and imaginary (ε_i) components of the dielectric constant decreased with dose, with ε_r remaining consistently higher than ε_i across the measured spectrum. These changes are attributed to radiation-induced defect states, which act as localized centers, reducing polarization and enhancing scattering losses. For 0.546 MeV β-electrons, the maximum transferable recoil energy is estimated to be approximately 16 eV for In atoms and 23 eV for Se atoms. These values are close to or below the typical displacement-threshold energy range reported for many solids. Therefore, the observed optical changes should not be attributed solely to direct knock-on displacement damage. Instead, ionization, electronic excitation, charge trapping, defect-state modification, weak bond rearrangement, and possible local structural relaxation are considered to be the dominant mechanisms under the present irradiation conditions. The radiation sensitivity of the obtained optical constants and dielectric parameters indicate that InSe thin films can be effectively used not only in optoelectronic and photovoltaic devices but also in radiation dosimetry and sensor applications where ionizing radiation is used.

Author contributions

CRediT: **Cansu Emir:** Data curation, Formal analysis, Investigation, Supervision, Writing – original draft, Writing – review & editing; **Sema Bilge Ocak:** Formal analysis, Methodology, Project administration, Resources, Supervision, Writing – original draft, Writing – review & editing; **Adem Tataroğlu:** Data curation, Investigation, Methodology, Writing – original draft, Writing – review & editing; **Uğur Gökmen:** Data curation, Formal analysis, Methodology, Resources, Writing – original draft.

Disclosure statement

No potential conflict of interest was reported by the author(s).

Funding

The authors would like to express their gratitude to the Scientific Research Projects Office of Gazi University, Türkiye [project number: FGA-2025–10402], for its financial support.

Data availability statement

The experimental data underlying this study are available from the corresponding author on reasonable request.

Declarations

The authors declare no competing interests.

References

[1] Yang Z, Hao J. Recent progress in 2D layered III–VI semiconductors and their heterostructures for optoelectronic device applications. Adv Mater Technol. 2019;4(8):1900108. doi: 10.1002/admt.201900108

[2] Zhang D, Wang B, Gan Y et al. New layered II–III–VI semiconductors: promising materials for high performance solar cells. J Phys Chem C. 2024;128(4):1582–1590. doi: 10.1021/acs.jpcc.3c07113

[3] Raksa P, Boon-On P, Ponhan W et al. Impact of potassium doping on the physical properties of cadmium sulfide thin films prepared by sol-gel screen printing technique. Ceram Int. 2026;52(11):17905–17924. doi: 10.1016/j.ceramint.2026.02.369

[4] Nedkun P, Sangsai P, Wongrat E et al. Post-annealing effects on the structural and optical properties of nickel vanadate thin films. Mater Lett. 2026;411:140324. doi: 10.1016/j.matlet.2026.140324

[5] van Gog H, Li W-F, Fang C et al. Thermal stability and electronic and magnetic properties of atomically thin 2D transition metal oxides. npj 2D Mater Appl. 2019;3(1):18. doi: 10.1038/s41699-019-0100-z

[6] Molas MR, Tyurnina AV, Z'olyomi V et al. Raman spectroscopy of GaSe and InSe post-transition metal chalcogenides layers. Faraday Discuss. 2021;227:163–170. doi: 10.1039/D0FD00007H

[7] Xie J, Zhang L. Optical emission enhancement of bent InSe thin films. Sci China Inf Sci. 2021;64(4):140405. doi: 10.1007/s11432-020-3149-2

[8] Tanabe T, Tang C, Sato Y et al. Direct determination of the interlayer van der Waals bonding force in 2D indium selenide semiconductor crystal. J Appl Phys. 2018;123(24):245107. doi: 10.1063/1.5024313

[9] Grimaldi I, Gerace T, Pipita MM et al. Structural investigation of InSe layered semiconductors. Solid State Commun. 2020;311:138555. doi: 10.1016/j.ssc.2020.113855

[10] Boukhvalov DW, Gürbulak B, Duman S et al. The advent of indium selenide: synthesis, electronic properties, ambient stability and applications. Nanomaterials. 2017;7(11):372. doi: 10.3390/nano7110372

[11] Politano A, Campi D, Cattelan M et al. Indium selenide: an insight into electronic band structure and surface excitations. Sci Rep. 2017;7(1):3445. doi: 10.1038/s41598-017-03186-x

[12] Du Y, Wang M, Ye X et al. Advances in the field of graphene-based composites for energy-storage applications. Crystals. 2023;13(6):912. doi: 10.3390/cryst13060912

[13] Darwish AAA. Photo induced effect in nanostructured InSe thin films for photonic applications. Opt Commun. 2014;310:104–108. doi: 10.1016/j.optcom.2013.07.064

[14] Singh H, Singh P, Singh R et al. Composition dependent structural phase transition and optical band gap tuning in InSe thin films. Heliyon. 2019;5(11):e02933. doi: 10.1016/j.heliyon.2019.e02933

[15] Boolchandani S, Srivastava S, Vijay YK. Preparation of InSe thin films by thermal evaporation method and their characterization: structural, optical, and thermoelectrical properties. J Nanotechnol. 2018;2018:9380573.

[16] Tripathi SK. Irradiation induced changes in semiconducting thin films. Defect Diffus Forum. 2013;341:181–210. doi: 10.4028/www.scientific.net/DDF.341.181

[17] Arshak K, Korostynska O. Response of metal oxide thin film structures to radiation. Mater Sci Eng B. 2006;133(1–3):1–7. doi: 10.1016/j.mseb.2006.06.012

[18] Vavilov VS, Ukhin NA. Radiation effects in semiconductors and semiconductor devices. New York: Springer; 1977.

[19] Selim NS, El-Marakby SM. Radiation-induced changes in the optical properties of hemoglobin molecule. Spectrochim Acta Part A. 2010;76(1):56–61. doi: 10.1016/j.saa.2010.02.046

[20] Sharma SL, Maity TK. Effect of gamma radiation on electrical and optical properties of (TeO_2)0·9 (In_2O3) 0·1 thin films. Bull Mater Sci. 2011;34(1):61–69. doi: 10.1007/s12034-011-0027-2

[21] Eisa MH. Effects of beta-ray irradiation on optical properties of PbO thin films. Mater Sci Semicond Process. 2020;110:104966. doi: 10.1016/j.mssp.2020.104966

[22] Nefzi C, Beji N, Souli M et al. Effect of gamma-irradiation on optical, structural and electrical properties of In_2O_3: f thin films for photocatalysis application. Opt Laser Technol. 2019;112:85–92. doi: 10.1016/j.optlastec.2018.11.010

[23] El-Saady AA, Roushdy N, Farag AAM et al. Influence of gamma-irradiation on the structural, morphological, and optical properties of β-H_2Pc nanocrystalline films: implications for optoelectronic applications. J Electron Mater. 2023;52(12):8001–8018. doi: 10.1007/s11664-023-10703-4

[24] Wooten F. Optical properties of solids. New York: Academic Press; 1972.
[25] Pankove JI. Optical processes in semiconductors. New York: Dover Publications; 1975.
[26] Singh J. Optical properties of condensed matter and applications. Chichester (UK): John Wiley & Sons; 2006.
[27] El-Mesady IA, Rammah YS, Abdalla AM et al. Gamma irradiation effect towards photoluminescence and optical properties of Makrofol DE 6–2. Radiat Phys Chem. 2020;168:108578. doi: 10.1016/j.radphyschem.2019.108578
[28] Madani M, El-Sayed SM. Radiation effects on optical properties of ethylene vinyl acetate copolymer films. J Macromol Sci Phys. 2007;46(3):441–451. doi: 10.1080/00222340701257554
[29] Abd El-Raheem MM, Hassan HE, Wakkad MM et al. The effects of gamma irradiation on the optical and electrical properties of melt-quench $Ge_{18}Bi_4Se_{78}$ chalcogenide glass. Inf Sci Lett. 2022;11:971–978.
[30] Emir C, Tataroğlu A, Coşkun E et al. Structural and optical properties of interfacial InSe thin film. ACS Omega. 2024;9:7588–7596. doi: 10.1021/acsomega.3c06600
[31] Hassan Salman S, Ali SM, Sarhan Ahmed G. Study of the effect of annealing on structural and optical properties of indium selenide (InSe) thin films prepared by vacuum thermal evaporation technique. J Phys Conf Ser. 2021;1879(3):032058. doi: 10.1088/1742-6596/1879/3/032058
[32] Hossain J, Julkarnain M, Sharif KS et al. Optical properties of e-beam evaporated indium selenide (InSe) thin films. J Sci Res Rep. 2014;3(12):1642–1655. doi: 10.9734/JSRR/2014/7658
[33] Abusaleh BA, Elimat ZM, Alzubi RI et al. Effects of gamma radiation on the optical properties of ultrafine iron particle/polystyrene composites. Radiat Eff Defects Solids. 2024;179(9–10):1259–1283. doi: 10.1080/10420150.2024.2335222
[34] Qasrawi AF. Temperature dependence of the band gap, refractive index and single-oscillator parameters of amorphous indium selenide thin films. Opt Mater. 2007;29(12):1751–1755. doi: 10.1016/j.optmat.2006.09.009
[35] Abd Al-Sahib Wadi H. Effect of laser radiation on optical properties of CdO thin films. J Sci Technol. 2017;9:1–5.
[36] Addayeva Z, Muradov M, Eyvazova G et al. Effect of temperature and gamma irradiation on dielectric properties of FeGaInS4/PVA composites. RSC Adv. 2026;16(1):586–603. doi: 10.1039/D5RA08220J
[37] Husein Qwasmeh AA, Abu Saleh BA, Al-Tweissi M et al. Effects of gamma irradiation on optical properties of poly(ethylene oxide) thin films doped with potassium iodide. J Compos Sci. 2023;7(5):194. doi: 10.3390/jcs7050194
[38] Narayanan KL, Vijayakumar KP, Nair KGM et al. Effect of irradiation-induced disorder on the optical absorption spectra of CdS thin films. Physica B. 1997;240(1–2):8–12. doi: 10.1016/S0921-4526(97)00428-6
[39] Abdelhamid SM, Dongol M, Elhady AF et al. Impact of transparent conducting substrates on structural and optical of titanium(IV) phthalocyanine dichloride (TiPcCl2) thin films. Discov Appl Sci. 2024;6(2):45. doi: 10.1007/s42452-024-05638-2
[40] Tauc J. Amorphous and liquid semiconductorseff. New York: Plenum Press; 1974.
[41] Klein J, Kampermann L, Mockenhaupt B et al. Limitations of the Tauc plot method. Adv Funct Mater. 2023;33(47):2304523. doi: 10.1002/adfm.202304523
[42] Harynski Ł, Olejnik A, Grochowska K et al. A facile method for Tauc exponent and corresponding electronic transitions determination in semiconductors directly from UV–Vis spectroscopy data. Opt Mater. 2022;127:112205. doi: 10.1016/j.optmat.2022.112205
[43] Chaiworn P, Kambut A, Pluengphon P et al. Aluminum antimony alloy overlayers synthesized using the electrodeposition method: investigation of structural, optical, electrical properties, and DFT calculation. Semicond Sci Technol. 2024;39(11):115012. doi: 10.1088/1361-6641/ad7d88
[44] El-Nahass MM, Saleh A-BA, Darwish AAA et al. Optical properties of nanostructured InSe thin films. Opt Commun. 2012;285(6):1221–1224. doi: 10.1016/j.optcom.2011.11.031
[45] El- Damhogi DG, Elesh E, Ibrahim AH et al. The impact of radiation on the morphological, structural properties, linear and nonlinear optical parameters of gallium phthalocyanine chloride thin films for optoelectronic devices. Radiat Phys Chem. 2022;195:110060. doi: 10.1016/j.radphyschem.2022.110060
[46] Suwannakham N, Tubtimtae A, Wongrat E. Structural, linear/non-linear optical, optoelectrical, and electrical properties of novel crystalline antimony-doped tin oxide thin films synthesized by the chemical deposition method. Physica B. 2023;649:414440. doi: 10.1016/j.physb.2022.414440
[47] Reddy RR, Rama Gopal K, Narasimhulu K et al. Correlation between optical electronegativity and refractive index of ternary chalcopyrites, semiconductors, insulators, oxides and alkali halides. Opt Mater. 2008;31(2):209–212. doi: 10.1016/j.optmat.2008.03.010
[48] Fleifil SS, Hassan QMA, Dhumad AM et al. Gamma radiation effect on the optical linear and nonlinear properties of PVA with trypan blue film. Radiat Eff Defects Solids. 2023;178(5–6):699–723. doi: 10.1080/10420150.2023.2177995
[49] El Hachmi A, Manoun B. Complex dielectric, electric modulus, impedance, and optical conductivity of Sr3 $-x$Pb$x$$Fe_2TeO_9$ (x =1.50, 1.88 and 2.17). Int J Mater Res. 2023;114(2):100–110. doi: 10.1515/ijmr-2022-0189
[50] Arbab AI, Sherfee FO. Validation of optical conductivity and tailing parameter. EPL. 2024;147(4):46003. doi: 10.1209/0295-5075/ad69be
[51] Attia Abuelwafa A, Elnobi S, Yamada I et al. Studying the linear and nonlinear optical properties of trifluoroethoxy-coated zinc phthalocyanine ((4TFEO) 4-ZnPc) thin films. Opt Mater. 2022;123:111850. doi: 10.1016/j.optmat.2021.111850
[52] Kumar Bhunia A, Sekhar Pradhan S, Bhunia K et al. Study of the optical properties and frequencydependent electrical modulus spectrum to the analysis of electric relaxation and conductivity effect in zinc oxide nanoparticles. J Mater Sci Mater Electron. 2021;32(17):22561–22578. doi: 10.1007/s10854-021-06742-4
[53] Güllü O, Türkeri M, Tataroğlu A. Electrical and optical characterization of Al/MgO/p-Si (MIS) diode with magnesium oxide thin films by spraying method. Solid State Commun. 2025;403:115992.

[54] Ganesh V, Haritha L, Elhosiny Ali H et al. The detailed calculations of optical properties of indium-doped CdO nanostructured films using Kramers-Kronig relations. J Non-Cryst Solids. 2021;552:120454. doi: 10.1016/j.jnoncrysol.2020.120454

[55] Bourguiba F, Dhahri A, Tahri T et al. Structural, optical spectroscopy, optical conductivity and dielectric properties of BaTi0.5(Fe0.33W0.17)O3 perovskite ceramic. Bull Mater Sci. 2016;39(7):1765–1774. doi: 10.1007/s12034-016-1305-9

[56] Attia Abuelwafa A, Soga T, Elnobi S. Optimized structural, optical, and electrical properties of spin-coated Pt(II) octaethylporphyrin thin films for optoelectronic applications. Optik. 2023;295:171538. doi: 10.1016/j.ijleo.2023.171538

[57] Lemziouka H, Boutahar A, Moubah R et al. Synthesis, structural, optical and dispersion parameters of La-doped spinel zinc ferrites ZnFe2-xLaxo4 (x = 0.00, 0.001, 0.005, 0.01 and 0.015). Vacuum. 2020;182:109780. doi: 10.1016/j.vacuum.2020.109780

[58] Elnobi S, Abd El-Sadek MS, Yahia IS et al. Correlation between structural, morphological, and optical properties of spin-coated poly (2,5-di(hexyloxy) cyanoterephthalylidene) (CN-PPV) thin films. J Mater Sci Mater Electron. 2022;33(28):22092–22102. doi: 10.1007/s10854-022-08977-1